International Journal of Automotive Technology, Vol. ?, No. ?, pp. ?−?(year)

APPARATUS FOR IDENTIFICATION OF FRICTIONAL AND THERMAL CHARACTERISTICS OF A WET CLUTCH

Seungin Shin[1)], Dong-Hyun Kim[1)] and Seibum B. Choi[1)*]

[1)] Department of Mechanical Engineering, KAIST, Daejeon 34141, Korea

(*Received date ; Revised date ; Accepted date*) * Please leave blank

ABSTRACT− This paper describes the configuration of an apparatus for fundamental research on frictional characteristics for wet clutch control. The friction coefficient usually varies depending on the friction speed, the temperature of the friction surface, and the pressing force. The design and configuration for accurately measuring each major variable were presented. There is a fluid circulation system to implement an environment similar to an actual wet clutch system. It is designed to analyze the friction characteristics by maintaining the fluid film dynamics in a steady-state or to simulate the clutch engagement by controlling the speed of the motor. A friction coefficient map for any multi-disc clutch could be obtained with the presented apparatus, and a map of an automatic transmission clutch is obtained as an example. The experimental result shows the variables of the friction coefficient were the friction speed and the temperature of the friction surface, and in particular, it increased linearly with the temperature of the friction surface within the experimental range.

KEY WORDS : Wet clutch, Friction coefficient, Clutch temperature, Test bench

NOMENCLATURE

x_p : piston position, m
h : nominal separation between clutches, m
N_c : number of clutches
z : film thickness, m
β : asperity tip radius, m
σ : RMS roughness of friction material, m
p_h : hydrodynamic pressure, Pa
p_c : contact pressure, Pa
R_{eff}: torque effective radius of clutch, m
v : mean slip speed of clutch, m/s
R_o : outer radius of clutch disk, m
R_i : inner radius of the clutch disk, m
$\Delta\omega$: clutch rotational slip speed, rad/s
τ : clutch torque, Nm
τ_c : asperity contact torque, Nm
τ_v : viscous torque, Nm
μ_f : asperity friction coefficient
μ_v : dynamic viscosity of the fluid, mPa·s
$\bar{h}$: average fluid film thickness, m
T : mean temperature of friction surfaces of clutches, °C
μ_{v1}, μ_{v3} : dynamic viscosity parameters, mPa·s
μ_{v2}, μ_{v4} : dynamic viscosity parameters, K^{-1}
m : mass, kg
c_p : specific heat capacity, J·kg^{-1}·K^{-1}
k_1 generalized thermal conductivity of convection, W/K
k_2 generalized thermal conductivity of conduction, W/K

1. INTRODUCTION

Research on the improvement of fuel efficiency and riding comfort in the vehicle field is continuing. The transmission is directly related to the fuel efficiency of an internal combustion engine vehicle, and an undesired impact during vehicle launch or gear shifting may cause discomfort to the driver. There are transmissions using various mechanisms such as automatic transmission (AT) using planetary gears, dual-clutch transmission (DCT), and continuously variable transmission (CVT), and each is used based on different advantages and disadvantages. Among them, the AT uses a hydraulic system and a wet

* *Corresponding author*. e-mail: sbchoi@kaist.ac.kr

clutch and has a very smooth gear shifting thanks to the torque converter.

Although the proportion of AT in the total vehicle is decreasing, the need for precise control of the wet clutch is increasing. The operation of the fluid coupling is being developed to minimize the operation due to the disadvantage that inevitably consumes energy. When the use of the fluid coupling is minimized, the control of the clutch during gear shifting needs to be more precise to prevent shift shock, shudder and excessive slip. At the same time, the transmission has a trend of being multi-speed, such as 8-speed and 10-speed, and accordingly, a lot of shifting occurs during a drive. The gear shift jerk should also be reduced so that the driver will not complain of discomfort. Even in hybrid vehicles, a motor is used instead of a torque converter. The number of hybrid vehicles will increase according to the global demand for fuel efficiency improvement, and the wellmade product should be supported by its control performance. Wet clutches are used in AT as well as wet dual-clutch transmission (wDCT), electrified AT (hybrid vehicle) and limited-slip differentials (LSD).

The driver's discomfort that occurs in clutch engagement can be resolved by precise control of the clutch. The engagement process is very short in time, and since the measured values are also very limited in commercialized vehicles, it is difficult to expect good performance with feedback (FB) control. Usually, there is no pressure sensor, torque sensor cannot be installed, and clutch slip which is the only measurement is indirectly measured in AT. The clutch slip is calculated with the kinematics of the planetary gear set and shaft, so the accuracy is not guaranteed. Therefore, the feed-forward (FF) control, which creates a high-accuracy and simple model and generates a system input using the inverse model, is suitable for clutch engagement control due to its guaranteeing transient control performance.

Open-loop control prepared for all situations by tuning the time-series input can cause an explosive increase in development man-hours. The physical variable that dominates the clutch engagement process is the friction coefficient, which is known to be affected by many variables. After Coulomb (Coulomb, 1821) proposed the concept of the coefficient of friction, research results are showing that it is affected by various variables such as the pressing force, the temperature of the friction surface, and the friction speed (Holgerson and Lundberg, 1999a;Holgerson, 1997; Marklund and Larsson, 2008; Marklund *et al*, 2007; Ivanovic *et al*, 2009; Ivanovic *et al*, 2012; Maki *et al*, 2005). Studies have mainly focused on two friction materials. The first is a paper-based material friction lining (Holgerson and Lundberg, 1999a;Holgerson, 1997; Holgerson and Lundberg, 1999b; Li *et al*, 2015, Li *et al*, 2014; Li *et at*, 2017; Lingesten *et al*, 2012) generally used in AT clutches and a brass material friction lining (Marklund and Larsson, 2008; Marklund *et al*, 2007; Ivanovic *et al*, 2009; Ivanovic *et al*, 2012; Maki *et al*, 2005) used in limited-slip differentials. This study deals with paper-based materials. The friction coefficient static map is a model in which the friction coefficient is assumed to vary depending on several variables, and the value is determined according to the current value of each variable. On the other hand, the dynamic model is a model that assumes that the differential of variables such as the amount of change in the pressing force is also a variable that determines the friction coefficient. Each has its pros and cons, and the dynamic model usually has relatively many characteristic values to know, and a lot of research on the target clutch is needed, but the results are in good agreement with the model and experimental results. Static maps are simple and do not fit well in some conditions. There is a study that shows that it fits well at high pressure changes and high speeds (Deur *et al*, 2005).

There have been studies to improve automatic transmission control performance by applying the friction coefficient model. When the friction coefficient is largely changed by temperature variation, if no compensation is done, the control performance may be greatly reduced (Maki 2005). There was also a study to extend the clutch life by analyzing the friction characteristics of the clutch (Holgerson, 2000). They used a simple technique of ramping down the pressure on the clutch at a specific point in time to achieve a smooth engagement and prevent excessive clutch temperature increase. There was also a study to control the precise clutch torque by assuming that there is uncertainty in the friction coefficient during DCT shift control and configuring a dynamic torque observer that adapts the uncertainty coefficient (Kim and Choi, 2020). It is important to know the clutch friction coefficient accurately to perform model-based shift control such as a study for generating slip speed reference during shift control of a transmission (Park and Choi, 2021).

The SAE machine No 2 (SAE International, 1991), which has been widely used for clutch characteristics experiments, has a major difference from the actual automatic transmission situation (Holgerson and Lundberg, 1999a). SAE machine no. 2 is basically an inertia dynamometer. In its clutch engagement phase, only the inertial force of the rotating body exists and there is no motor torque. Only the clutch torque exists as braking torque and can only create a deceleration scenario. However, in reality, in the case of the torque phase of gear shifting, engine torque is applied and the clutch slip speed may be kept constant or even increased. For more precise experiments, the capacity of the motor torque should be greater than that of the clutch, so that the rotation speed can be controlled as desired.

In this paper, we present an apparatus for analyzing the friction characteristics of a wet clutch. The friction

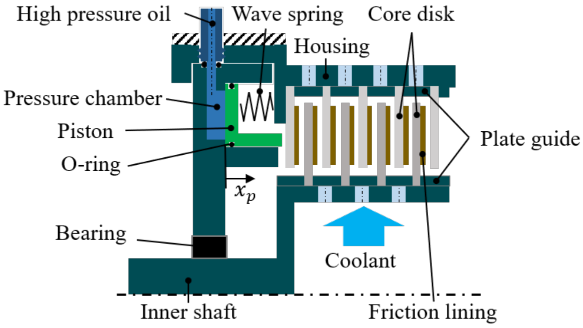

Figure 1. Schematic diagram of a multi-plate clutch system

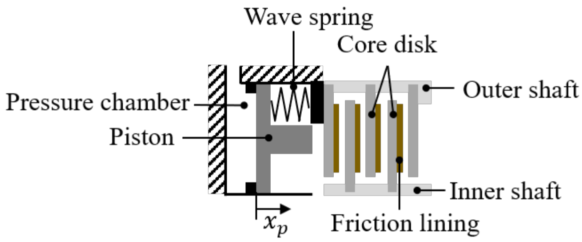

Figure 2. Simplified schematic diagram.

surface temperature, slip speed, and applied force on the clutch, which are the major variables of friction, can be measured, and the lubrication and cooling fluid is circulated. Section 2 presents the modeling of the entire system, and Section 3 describes the configuration of the experimental apparatus that can analyze the friction characteristics. Finally, the experimental results that can be obtained with the proposed apparatus are shown.

2. MODEL

The wet multi-plate clutch system operates with a hydraulic actuator, and the schematic diagram of the cross-section is drawn in the Fig. 1. Working fluid enters the pressure chamber and pushes the piston to bring the multi-plate clutches into contact, and eventually friction occurs. The higher the pressure in the chamber, the harder the piston squeezes the clutches, and the greater the friction torque. A simplified schematic diagram is drawn in Fig. 2. Spring puts the piston back in place when pressure is relieved in the pressure chamber. The inner and outer shafts are illustrated, and it is the role of the clutch to connect these two shafts by friction torque.

Figure 3 shows the transition of the lubrication regime and the deformation of the friction material according to the position of the piston.

The nominal separation h, the distance from the average height of the rough-surface friction lining to the smooth steel core disk, and the piston position x_p have a static relationship as follows:

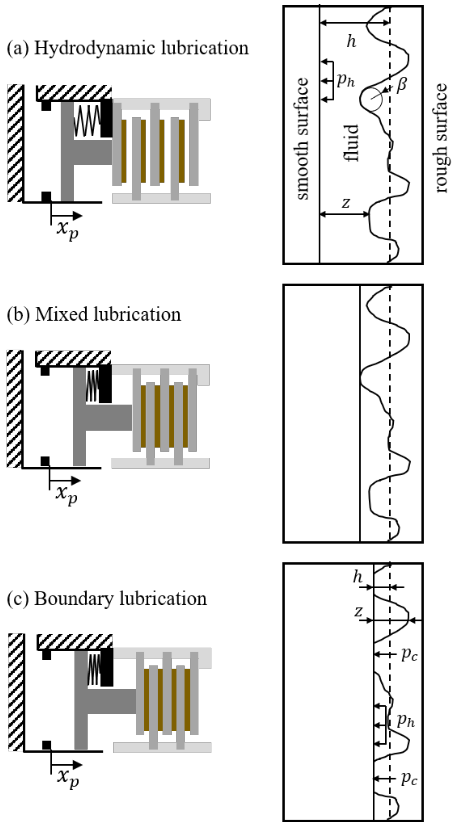

Figure 3. Deformation of the asperity tip and lubricated friction in the engagement process.

$$h = \frac{x_{p,h0} - x_p}{N_c} \tag{1}$$

where $x_{p,h0}$ is the position of the piston when nominal separation is 0, and N_c is the number of clutches of the multi-disc clutch.

As shown in Fig. 3(a), when the clutches are separated, there is no contact between the friction lining material and the steel core disk, and it is a hydrodynamic lubrication state. In this state, there is no asperity contact friction, only viscous friction. As the piston approaches and contact occurs, it becomes a mixed lubrication state as shown in Fig. 3(b), and eventually reaches a boundary lubrication state as shown in Fig. 3(c).

Assuming that the height z of the asperity tip is a Gaussian distribution over the entire surface, we can define the relationship between nominal separation h and average fluid film thickness $\bar{h}$ when deformed. (Patir and Cheng, 1979):

$$\bar{h} = \frac{h}{2}\left[1 + \operatorname{erf}\left(\frac{h}{\sqrt{2}\sigma}\right)\right] + \frac{\sigma}{\sqrt{2\pi}} e^{-\left(\frac{h}{\sqrt{2}\sigma}\right)^2} \tag{2}$$

where erf is the error function of Gaussian distribution.

2.1. Friction model

The friction is the sum of the viscous friction and the asperity contact friction.
The torque effective radius R_{eff} and mean slip speed v of the clutch are given by:

$$R_{eff} = \frac{2}{3} \cdot \frac{R_o^3 - R_i^3}{R_o^2 - R_i^2} \quad (1)$$

$$v = R_{eff} \Delta\omega \quad (2)$$

where R_o and R_i are the outer and inner radii of the clutch disk, and $\Delta\omega$ is the clutch rotational slip speed. Wet clutch torque τ consists of asperity contact torque τ_c and viscous torque τ_v:

$$\tau = \tau_c + \tau_v \quad (3)$$

$$\tau_c(v, T, F_c) = R_{eff} N_c \mu_f(v, T) F_c \quad (4)$$

$$\tau_v(v, T, \bar{h}) = R_{eff} N_c \mu_v(T) A_f \frac{v}{\bar{h}} \quad (5)$$

where T is the mean temperature of the friction surfaces of the clutches, N_c is the number of clutches, μ_f and μ_v are the asperity friction coefficient and dynamic viscosity of the oil respectively, and $\bar{h}$ is the average fluid film thickness. From (3,4,5), we have

$$\tau(v, T, F_c, \bar{h}) = R_{eff} N_c \left(\mu_f(v, T) F_c + \mu_v(T) A_f \frac{v}{\bar{h}} \right) \quad (6)$$

2.2. Dynamic viscosity

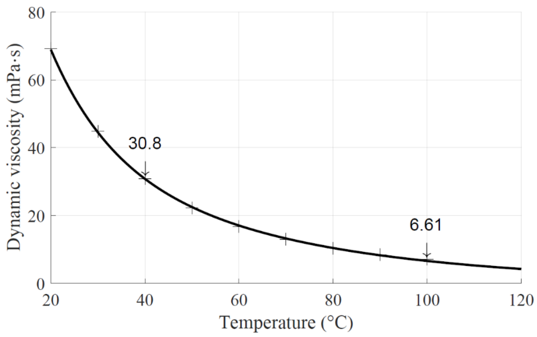

Figure 3. Dynamic viscosity μ_v of ATF.

The dynamic viscosity μ_v of ATF is a function of temperature. Its value is denoted by + and was fitted as the sum of two exponential functions as shown in Fig. 3. The specific values vary from manufacturer to manufacturer.

$$\mu_v(T) = \mu_{v1} e^{\mu_{v2} T} + \mu_{v3} e^{\mu_{v4} T} \quad (7)$$

where μ_{v1} to μ_{v4} are dynamic viscosity parameters.

2.3. Thermal dynamics

Considering real-time temperature estimation, it is difficult to estimate the surface temperature through finite element method (FEM). For control-oriented modeling, simple and fast dynamics model is required. The heat balance equation can be used to estimate the clutch friction surface temperature within an acceptable error range. The clutch core disk is generally made of steel, which is an excellent heat conductor, and is very thin, so it can be assumed that the temperature of the core disk is the same overall. Also, for the single-sided clutch, it can be assumed that the temperature of the steel core and the lining are also the same (Yang *et al*, 1995). Therefore, the entire clutch pack can be viewed as a lumped mass with uniform temperature.
The zero-dimensional heat balance equation for the clutch pack can be written as:

$$\left\{ (mc_p)_{lining} + (mc_p)_{core} \right\} N_c \dot{T} = \tau \Delta\omega - k_1 (T - T_{fluid}) - k_2 (T - T_{housing}) \quad (8)$$

where m and c_p are the mass and specific heat capacity of the friction lining and core plate, k_1 and k_2 are the generalized thermal conductivity of convection from the clutch pack to the cooling oil and conduction to the housing, respectively, and T_{fluid} and $T_{housing}$ are the temperature of the oil reservoir and the temperature of the structures in direct contact with the clutches. In general, the two temperatures are the same in an actual transmission, but in this research, they differed due to structural limitations and were measured for analysis. The thermal conductivity k_1 and k_2 were obtained experimentally and analyzed below.

3. TEST RIG

The experimental equipment to obtain the static map of the clutch friction coefficient requires the measurement of the clutch slip speed, the pressing force of the piston, the position of the piston, the clutch torque, and the temperature of the clutch. Each can be measured with an encoder, load cell, torque sensor, and thermistor, and the equipment composing it is shown in Fig. 4.
It is possible to use a hydraulic system as the real clutch system, but it is better to use a linear actuator with more detailed control in the test rig. Linear actuators are usually more linear and respond faster than hydraulic systems. Since the experimental equipment presented in this paper is to investigate the friction characteristics, a linear actuator was used to exclude unwanted phenomena.

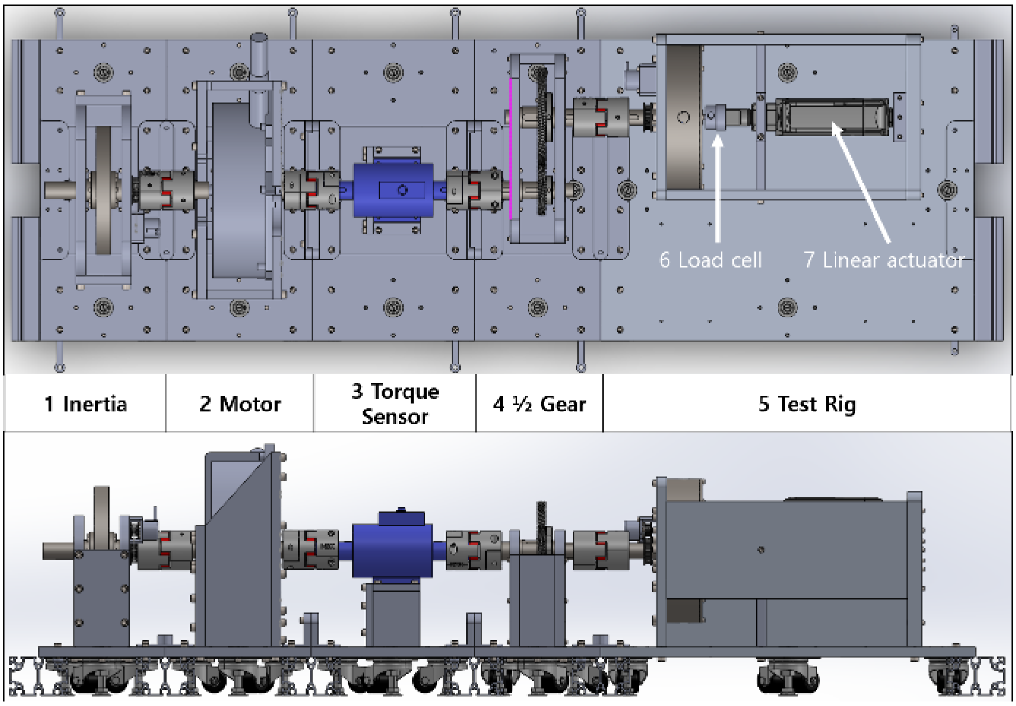

Figure 4. Test bench with wet clutch test rig.

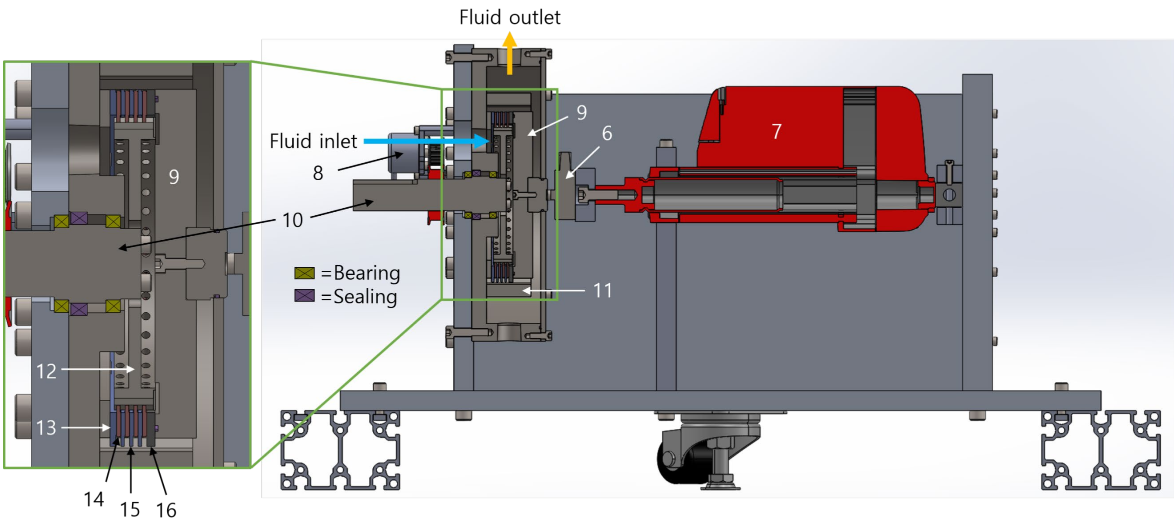

Figure 5. Cross-section of the test rig.

3.1. Organization

As illustrated in Fig. 4, the experimental equipment is mainly composed of motor 2, torque sensor 3, test rig 5, load cell 6, and linear actuator 7. The total length and width of the text bench are 2.05m and 0.62m. The motor controls the rotational speed of the entire rotating body including the inertia 1 so that the desired speed is maintained. In this study, a Hyundai Ioniq hybrid vehicle motor with a maximum output of 32 kW, a maximum torque of 120 Nm and a maximum speed of 6000 rpm was used. The range of the variable to be tested is 300 Nm, 3000 rpm, but in general, the operating range of the driving motor is insufficient in torque and larger in rotational speed than the range required for the clutch test. In this study, it was achieved through the 1/2 gear. The clutch (brake) used in the 2nd gear of Hyundai 8-speed rear-wheel-drive AT was used in the test. The linear

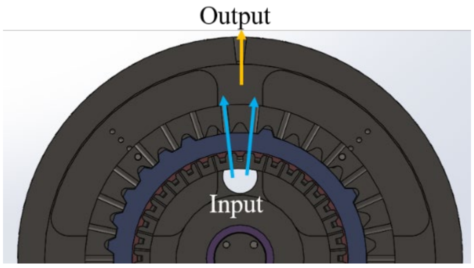

Figure 6. Axial cross-section of the test rig and fluid passage through the multi-plate clutch.

actuator is a 240 W linear motor that can generate a stall and dynamic pressing force of 16 kN. A load cell is attached to the end of the actuator to measure the pressing force of the piston. To get the desired rotational speed, the torque capacity of the motor and the motor controller need to cover the clutch torque range to be tested.

The motor torque passes through the gear 4, which is a torque amplifier, and reaches the clutches 14 and 15, where the braking torque actuated by the linear actuator takes place. The cross-section of the test rig is illustrated in Fig. 5: a rotary encoder 8 that measures the rotational speed of the input shaft 10; a piston 9 that transmits the pressing force of the linear actuator; an outer-guide 11, which is coupled to the outer-toothed clutches 15 and fixed to the housing and an inner-guide 12, which is coupled with the inner-toothed clutches 14 and fixed with the input shaft; and protection plates 13 and 16 are presented. The length of the test rig module is 0.77 m and the diameter of the cylindrical housing enclosing the clutches is 0.30 m. Inner and outer guides were machined to give the clutches a DOF along the axial direction. Oil flows into the rig through an inlet, passes between the gaps and the clutch grooves, cools the clutch, and exits through the outlet to reach the reservoir. They are depicted in Fig. 6, where the axial section is drawn. Only a few arrows are shown for simplicity, and the fluid flows in all directions through the clutch groove. As the outlet is higher than the inlet, the rig is filled with oil. The level of oil filling in the chamber is determined by the position of the outlet.

Figure 7 shows the multi-plate clutches, the input shaft, and the connecting serrated jig inside the test rig. As shown in Fig. 8, the clutch with teeth on the inside and outside overlap alternately to form a multi-plate clutch.

The guides for connecting the clutches with the input shaft and the housing are shown in Fig. 9. Their serrated surfaces were machined by electric discharge machining and CNC. Radial holes were drilled to allow cooling fluid to pass through the clutches.

The guides allow axial translation of the clutches and do not allow rotation. When the piston compresses the multi-plate clutch, frictional torque is generated. The torque is measured at the torque sensor after the gear module as shown in Fig. 4.

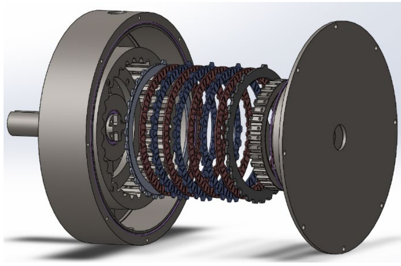

Figure 7. Multi-plate clutch inside the test rig.

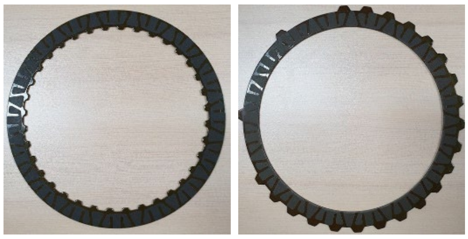

Figure 8. Single-sided clutches. Outer-toothed clutch disk (left). Inner-toothed clutch disk (right)

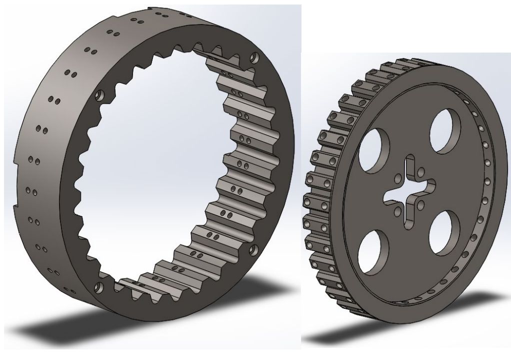

Figure 9. Clutch outer-guide and inner-guide.

Table 1. System parameters.

Number of clutches, N_c	8
Asperity tip radius, β	5×10^{-4} m
RMS roughness of friction material, σ	6×10^{-4} m
Torque effective radius of clutch, R_{eff}	0.07758 m
Outer radius of clutch disk, R_o	0.08315 m
Inner radius of clutch disk, R_i	0.07174 m
Core disk thickness	1.7 mm
Dynamic viscosity parameter 1, μ_1	150.2 mPa·s
Dynamic viscosity parameter 2, μ_2	-0.07838 K^{-1}
Dynamic viscosity parameter 3, μ_3	58.15 mPa·s
Dynamic viscosity parameter 4, μ_4	-0.02184 K^{-1}
Mass of paper-based lining material, m_{lining}	1.65 g
Mass of core disk, m_{core}	82.1 g
Specific heat capacity of lining material, $c_{p,lining}$	1500 $J \cdot kg^{-1} \cdot K^{-1}$
Specific heat capacity of core disk, $c_{p,core}$	500 $J \cdot kg^{-1} \cdot K^{-1}$
Generalized thermal conductivity by convection, k_1	122.2 W/K
Generalized thermal conductivity by conduction, k_2	39.94 W/K

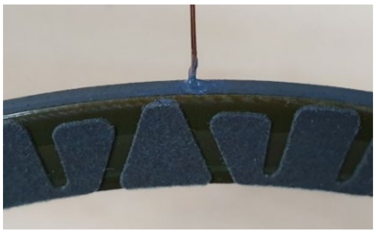

Figure 10. Installation of the thermistor in the clutch plate.

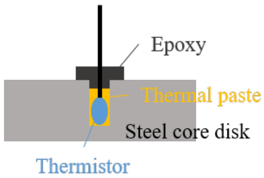

Figure 11. Insertion of the thermistor into the clutch core disk.

3.2. Thermistor implementation

Actual photos of the clutch are shown in Fig. 8. Their radii and thicknesses are given in Table 1. The outer-toothed clutches were fixed to the housing via an outer guide, so thermistors were inserted while the rotating inner-toothed clutches were not. As shown in Fig. 10, a thin thermistor with a diameter of 0.8mm was inserted in the center of the radial width of the clutch core disk. The gap between the hole and the thermistor was filled with liquid metal thermal paste with thermal conductivity of 73 W/mK for high conduction. Its opening was sealed with epoxy. The thermistor is inserted into the hole and the thermal paste and epoxy filled the gap as in Fig. 11. Since the thickness of the clutch is thin and the thermal conductivity of steel is high enough to assume that the thermistor measures the temperature of the friction surface. Its temperature measurement uncertainty is less than 1 percent.
A thermistor cannot be inserted into the inner toothed clutch that rotates with the input shaft, but the thermistor can only be inserted into the outer toothed clutches stationary on the housing.

3.3. Lubrication and cooling fluid circulation

In wet clutch systems, oil is circulated throughout the system to lubricate and cool the clutch. Because of this oil, viscous friction is generated, which makes control difficult, but it has the advantage of being resistant to frictional heat thanks to forced cooling. Similarly, in the experimental device, there is a controllable DC motor pump, its controller, and a flow rate sensor to realize fluid circulation, and through this, the cooling fluid is circulated through the clutches at a desired flow rate.

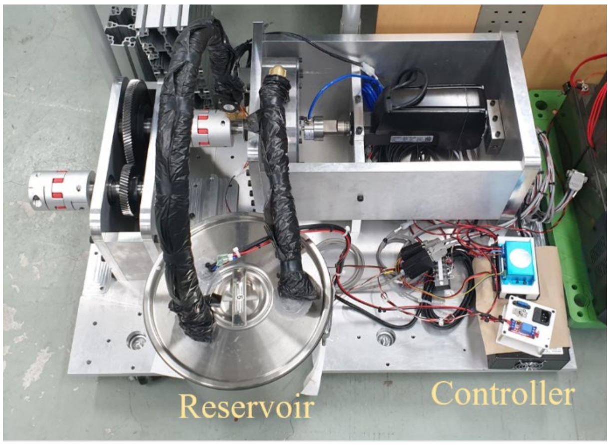

Figure 12. Real picture of test rig module.

Figure 12 shows the system including a reservoir. The flow rate was always maintained at 10 L/s in this study. The power of the pump should be at least 200W to maintain the flow rate. When the engine is idling, the oil flow rate is normally 10 to 20 L/s, and it can vary depending on the size of the pump and the engine speed. The pump capacity should also cover the range.
The clutch surface temperature affects the friction characteristics, and the reservoir and fluid temperatures affect the clutch initial temperature. In order to investigate the friction characteristics in a wide temperature range, the test rig should capable to maintain the reservoir temperature at a desired value. The greater the power of the heater, the faster the temperature of the reservoir is raised, allowing for faster experimentation. In this experiment, a ceramic heater with a power of 2000 W is installed inside the reservoir, and the temperature is decreased by natural cooling when desired.

4. EXPERIMENTS

Experiments that could not be done with the SAE machine no. 2 can be done with the proposed apparatus. It is possible to initiate rotation even with the initially applied load to the clutch and achieve the desired frictional speed as in Fig. 13. The fluid film steady-state was maintained to minimize oil squeezing, and the friction characteristics could be obtained using the equations in chapter 2. The final goal would be to find out the friction coefficient μ_f in (3) in various parameters, which is called a friction coefficient map.
During friction, torque, slip speed, clutch surface temperature, piston position, and applied force can be measured. When the friction speed is high, the temperature increases up to 14 seconds, and then the temperature decreases by convection cooling as the friction speed and heat energy input decrease. With this

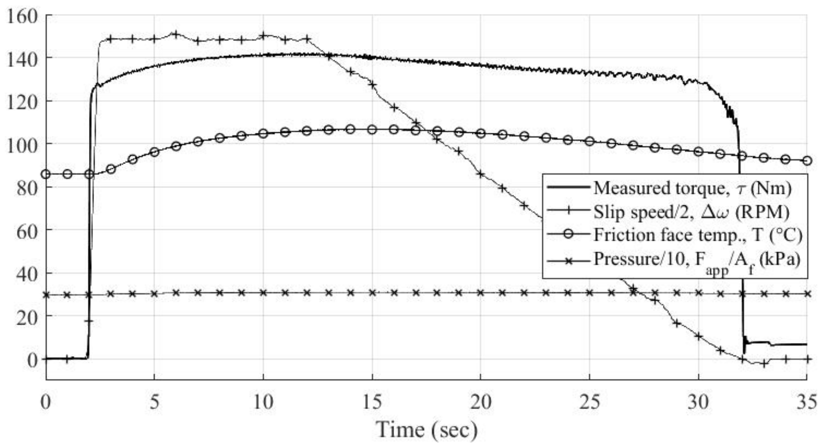

Figure 13. Experimental data available from test rig.

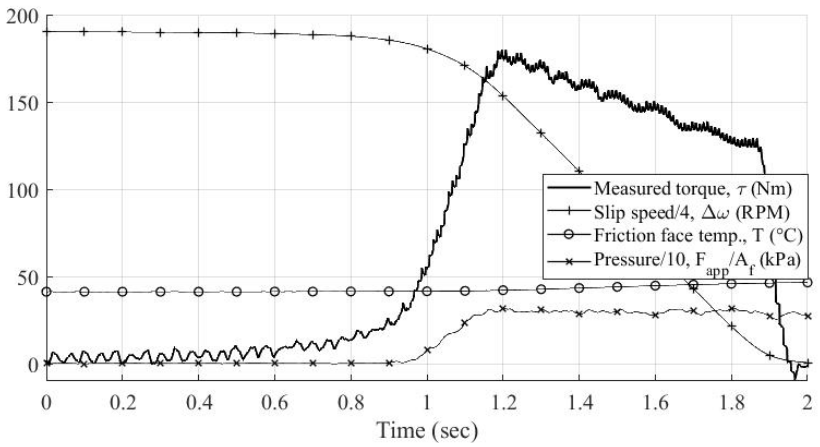

Figure 14. Experiments simulating clutch engagement.

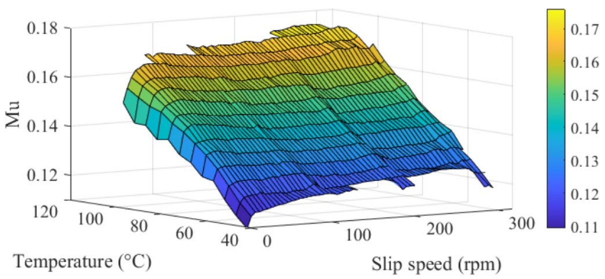

Figure 15. Friction coefficient map.

maintained and decreasing slip speed profile, friction torques at various temperature points can be obtained.

Fig. 13 is a typical example of an experiment using the proposed experimental apparatus. It is well known that the friction coefficient depends on the pressing force, the friction speed, and the temperature of the friction surface. As an experiment to find out the change in friction coefficient for three variables, it is desirable to fix two variables and change only one, but it was not easy to fix the temperature of the friction surface. The friction coefficient is affected by temperature but not by the rate of change of temperature, so it was varied slowly enough rather than fixed. The experiment consists of two sections. The first section increases the temperature while keeping the friction speed constant over 10 seconds, and the next section very slowly decreases the temperature and friction speed over 20 seconds. The pressing force should be kept constant from the start of the rotation to the end of the rotation to reject fluid film dynamics. In the experiment, a constant pressure of 300 kPa was used. In the first section, the friction speed was maintained at 300 rpm and the temperature was increased from 85°C to 108°C. The viscous torque (5) can be calculated from the torque measured during friction, the pressing force, the piston position and temperature, and the friction coefficient can also be calculated using (4).

The friction coefficient map in Fig. 15 can be obtained as a result of the experiments as in Fig. 13 for various initial frictional speeds, initial temperatures, and applied forces. The friction coefficient was not significantly affected by the applied force, was linear with temperature, and was negatively exponential to the slip speed within the experimental range.

The proposed apparatus is also possible to simulate the engagement process as shown in Fig. 14. The process was simulated over about 1 second, and the applied force was raised over 0.2 seconds and maintained at an arbitrary value to generate braking torque. The motor torque was controlled so that the rotational speed followed the slip reference. Here, a smoothed ramp-down curve is used as a slip reference. Similarly, the generation of viscous torque and asperity contact torque can be analyzed according to the pressure profile in the torque phase and inertia phase of gear shifting of AT.

5. CONCLUSION

We propose an apparatus and its design for testing the frictional characteristics of various wet clutches.

The major difference from SAE machine no. 2 is when designing experiments. The experiment can be designed more actively, so that the rotational speed and pressing force can be controlled in the time axis, unlike only the amount of rotational energy and piston pressure that can be adjusted only. However, variable controlling is clearly required because the friction characteristics are affected by various variables. The important point is that, in order to control the variables, not only the instantaneous clutch engagement experiment, but also the experimental device should be able to maintain a sustained or slowly varying variable condition.

A large-capacity motor is required for slip speed control, which makes it possible to maintain a fluid film steady-state or simulate the clutch engagement process. A thermistor inserted into the clutch measures the clutch surface temperature, which is an important variable in friction characteristics.

Products used in this study are listed in the appendix.

ACKNOWLEDGEMENT−This research was supported by the BK21+ program through the NRF funded by the Ministry of Education of Korea; the Technology Innovation Program (20010263) funded By the Ministry of Trade, Industry & Energy(MOTIE, Korea); the Technology Innovation Program (20014983) funded By the Ministry of Trade, Industry & Energy(MOTIE, Korea); the National Research Foundation of Korea(NRF) grant funded by the Korea government(MSIP) (No. 2020R1A2B5B01001531).

REFERENCES

1. Journals

Deur, J., Petric, J., Asgari, J., and Hrovat, D. (2005). Modeling of wet clutch engagement including a thorough experimental validation. *SAE trans.*, 1013-1028.

Holgerson, M. (1997). Apparatus for measurement of engagement characteristics of a wet clutch. *Wear* **213**, **1-2**, 140-147.

Holgerson, M. and Lundberg, J. (1999a). Engagement behaviour of a paper-based wet clutch Part 2: influence of temperature. *Proceedings of the Institution of Mechanical Engineers, Part D: J. of Automobile Engineering* **213**, **5**, 449-455.

Holgerson, M. and Lundberg, J. (1999b). Engagement behaviour of a paper-based wet clutch Part 1: influence of drive torque. *Proceedings of the Institution of Mechanical Engineers, Part D: J. of Automobile Engineering* **213**, **4**, 341-348.

Holgerson, M. (2000). Optimizing the smoothness and temperatures of a wet clutch engagement through control of the normal force and drive torque. *J. Trib.*, **122**, **1**, 119-123.

Ivanović, V., Herold, Z., Deur, J., Hancock, M. and Assadian, F. (2009). Experimental characterization of wet clutch friction behaviors including thermal dynamics. *SAE Int. J. of Engines* **2**, **1**, 1211-1220.

Ivanović, V., Deur, J., Herold, Z., Hancock, M. and Assadian, F. (2012). Modelling of electromechanically actuated active differential wet-clutch dynamics. *Proceedings of the Institution of Mechanical Engineers, Part D: J. of Automobile Engineering* **226**, **4**, 433-456.

Kim, S., and Choi, S. B. (2020). Cooperative control of drive motor and clutch for gear shift of hybrid electric vehicles with dual-clutch transmission. *IEEE/ASME Trans. on Mechatronics*, **25**, **3**, 1578-1588.

Li, M., Khonsari, M. M., McCarthy, D. M. C., and Lundin, J. (2014). Parametric analysis for a paper-based wet clutch with groove consideration. *Tribology Int.*, **80**, 222-233.

Li, M., Khonsari, M. M., McCarthy, D. M. C. and Lundin, J. (2015). On the wear prediction of the paper-based friction material in a wet clutch. *Wear* **334**, 56-66

Li, M., Khonsari, M. M., McCarthy, D. M. C., and Lundin, J. (2017). Parametric analysis of wear factors of a wet clutch friction material with different groove patterns. *Proceedings of the Institution of Mechanical Engineers, Part J: J. of Engineering Tribology*, **231**, **8**, 1056-1067.

Lingesten, N., Marklund, P., Höglund, E., Lund, M., Lundin, J., and Mäki, R. (2012). Apparatus for continuous wear measurements during wet clutch durability tests. *Wear*, **288**, 54-61.

Marklund, P., Maki, R., Larsson, R., Hoglund, E., Khonsari, M. M. and Jang, J. (2007). Thermal influence on torque transfer of wet clutches in limited slip differential applications. *Tribology int.* **40**, **5**, 876-884.

Marklund, P. and Larsson, R. (2008). Wet clutch friction characteristics obtained from simplified pin on disc test. *Tribology Int.* **41**, **9-10**, 824-830.

Park, J., and Choi, S. (2021). Optimization Method of Reference Slip Speed in Clutch Slip Engagement in Vehicle Powertrain. *Int. J. of Automotive Technology*, **22**, **1**, 55-67.

Patir, N., and Cheng, H. S. (1979). Application of average flow model to lubrication between rough sliding surfaces. *J. of Lubrication Technology* **101**, **2**, 220-229.

Yang, Y., Lam, R. C., Chen, Y. F., and Yabe, H. (1995). Modeling of heat transfer and fluid hydrodynamics for a multidisc wet clutch. *SAE trans.*, 1674-1688.

2. Books

Coulomb, C. A. (1821). *Théorie des machines simples en ayant égard au frottement de leurs parties et à la roideur des cordages*. Bachelier.

SAE International (Society). (2012). *SAE No. 2 Clutch Friction Test Machine Test Guidelines.* SAE J286 MAR2012. Society of Automotive Engineers.

4. Reports and User Guide

Mäki, R., Nyman, P., Olsson, R., and Ganemi, B. (2005). Measurement and characterization of anti-shudder properties in wet clutch applications. SAE Technical Paper. No. 2005-01-0878.

APPENDIX

Table Ⅰ. Products used in the study.

	Product (no.)	Manufacturer
Motor	32kW hybrid vehicle motor	Hyundai motor co.
Clutch	28-clutch of G80 RWD	Hyundai motor co.
Fluid	ATF SP-4 RR	Hyundai mobis
Linear actuator	Electrak HD24B160-0100ELP3NPS	Thomson
Linear actuator controller	ESCON 50/5	maxon
Load cell	MNC-2	CAS
NTC thermistor	NXFT15XH103FA	Murata
Thermal paste	Conductonaut	Thermal grizzly
Epoxy	Twin tube	J-B weld
Rotary encoder	E40S6-5000-3-T-5	Autonics
Torque sensor	HNR-50K	HAIAM ENG